

Theory of the mechanical response of focal adhesions to shear flow

This article has been downloaded from IOPscience. Please scroll down to see the full text article.

2010 J. Phys.: Condens. Matter 22 194111

(<http://iopscience.iop.org/0953-8984/22/19/194111>)

View [the table of contents for this issue](#), or go to the [journal homepage](#) for more

Download details:

IP Address: 129.252.86.83

The article was downloaded on 30/05/2010 at 08:03

Please note that [terms and conditions apply](#).

Theory of the mechanical response of focal adhesions to shear flow

Y Y Biton and S A Safran

Department of Materials and Interfaces, Weizmann Institute of Science, Rehovot 76100, Israel

E-mail: yoav.biton@weizmann.ac.il and sam.safran@weizmann.ac.il

Received 8 October 2009, in final form 7 January 2010

Published 26 April 2010

Online at stacks.iop.org/JPhysCM/22/194111

Abstract

The response of cells to shear flow is primarily determined by the asymmetry of the external forces and moments that are sensed by each member of a focal adhesion pair connected by a contractile stress fiber. In the theory presented here, we suggest a physical model in which each member of such a pair of focal adhesions is treated as an elastic body subject to both a myosin-activated contractile force and the shear stress induced by the external flow. The elastic response of a focal adhesion complex is much faster than the active cellular processes that determine the size of the associated focal adhesions and the direction of the complex relative to the imposed flow. Therefore, the complex attains its mechanical equilibrium configuration which may change because of the cellular activity. Our theory is based on the experimental observation that focal adhesions modulate their cross-sectional area in order to attain an optimal shear. Using this assumption, our elastic model shows that such a complex can passively change its orientation to align parallel to the direction of the flow.

(Some figures in this article are in colour only in the electronic version)

1. Introduction

Forces exerted by and on adherent cells are important for many physiological processes such as wound healing and tissue formation. Understanding the fundamental response of biological cells to mechanical stress is therefore an important challenge. Recent theoretical models [1, 2] predict the observed orientational response of cells to mechanical stress applied to the surrounding matrix [3]. The response of cells to curvature-imposed stress is treated theoretically in [4], which provides an explanation for the observed behavior of cells spread on a rigid cylindrical substrate [5, 6]. However, these models cannot be used to explain the orientational response of cells plated on a rigid substrate to shear flow. Many experimental studies of cellular response to shear flow are motivated by the need to understand the mechanics that governs the behavior of endothelial cells in the inner surface of blood vessels. These experiments show that these cells tend to align their stress fibers parallel to the direction of the flow [7–10]. In most *in vitro* experiments, a cell plated on a flat fixed substrate is subject to a laminar, fully developed, flow imposed in a uniform direction that is parallel to the basal surface of the cell. The experimental boundary conditions are chosen so that the shear imposed by the (Couette) flow

is constant and can be easily controlled by changing the volumetric flow rate.

Contractile cells are characterized by actin stress fibers in which tension is induced by myosin II molecular motors [11]. The stress is transmitted to the substrate by protein aggregates called focal adhesions. The stability, size, shape and dynamics of focal adhesions depend on the cytoskeletal tension as well as on externally applied forces; in the absence of force, the adhesions are no longer stable [12–15].

The active system that consists of a pair of focal adhesions connected by a contractile stress fiber is here referred to as a focal adhesion complex or, in short, a complex. The model presented is based on the experimentally observed [16, 17] tendency of focal adhesions to attain an optimal shear¹. We take this observation as an assumption that is employed in our model by constraining the values of the total force per unit cross-sectional area in each of the two focal adhesions to be equal. With this, the theory predicts that the free energy of deformation is minimal when the complex is aligned parallel to the direction of the flow. The theory also implies that this passive orientational response would not take place if either the

¹ An optimal shear in the sense that the free energy associated with the active changes in the size of a focal adhesion is minimized.

contractility of the stress fiber or the appropriate active change in the focal adhesions size are inhibited.

2. Basic assumptions

In the present work, we model each focal adhesion as an elastic body of cross-sectional area A . The adhesion height, ℓ , is the distance between the plane at which the adhesion meets the substrate and the (parallel) plane at which the adhesion intersects the stress fiber. Since this distance is small compared to the characteristic radius of the adhesion, we neglect bending deformations of the structure and take into account only shearing due to forces applied to the top of the cell. These external forces are assumed to act parallel to the basal surface of the cell. Because we are interested in the *response* of cells to shear flow, we take into account the forces that arise from the shear flow as well as the forces generated by the stress fibers through myosin-activated contractility.

Each of the focal adhesions included in the pair has one end attached to a substrate; its other end is connected to the stress fiber that joins the pair. In our model, we treat the stress fiber as a fixed contractile force that is exerted on each focal adhesion. Each focal adhesion is modeled as an elastic body whose size and shape can be actively adjusted by the cell in response to both contractile and external forces, such as flow-induced shear forces. A more realistic model, proposed in [18] and [19], suggests that the shear along the basal surface of a single focal adhesion² is a monotonically decreasing function of the distance from the edge connected to the stress fiber. However, for the purpose of investigating only the average response of a single complex to shear flow (and not the local response of the material comprising the focal adhesion), we approximate the shear to be homogeneous and equal to the mean value of the actual shear profile, i.e. the resultant force acting on a focal adhesion per unit area of the focal adhesion's basal surface. Accordingly, the displacement of the focal adhesion cross section that is parallel to the (rigid) planar substrate is taken to be a linear function of z , where z measures the distance from the basal plane. A three-dimensional schematic description of the model is shown in figure 1.

Focal adhesions at the two termini of a stress fiber are subject to dynamic processes related to their growth, saturation and decay [19, 20]. Such behavior, together with the possibility of disassembly and reassembly of focal adhesions and stress fibers, enable cells to reorient their stress fibers to a configuration in which the associated free energy of deformation can be minimal.

The experiments and theory (in the presence of contractility but not external shear flow) reported in [16] and [17] suggest that the interfacial area of a focal adhesion is proportional to the net force exerted on the focal adhesion³.

² The rat embryo fibroblasts used in the experiments reported in [19] were under no external forces (such as the forces result from a shear flow) other than the focal-adhesion–substrate anchoring forces.

³ The results reported in figure 5a of the article [16] show a linear relation between the applied force and cross-sectional area of a focal adhesion. Similar results are reported in figure 3H of [17] for cross-sectional areas greater than $1 \mu\text{m}^2$.

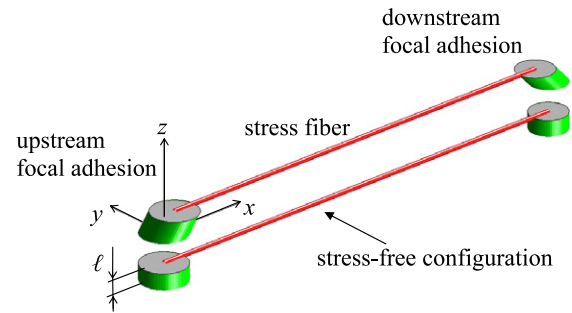


Figure 1. A 3D schematic description of the model. Each focal adhesion is shown as a deformed elastic body that has an (intrinsic) cylindrical shape when stress-free. The stress-free configuration of the focal adhesion complex is shown below a deformed configuration.

This finding may be interpreted in terms of cellular activity in which the larger size of a focal adhesion makes it possible for more stress fibers to integrate and result in a larger force. However, this interpretation implies that, when the sizes of the two focal adhesions in a complex are different, the contractile force may not be constant along a stress fiber. Such variability of the force along a stress fiber cannot exist if the stress fiber is in stable mechanical equilibrium in which its tension must be constant. In contrast, an alternative approach suggests that a cell regulates its activity to adjust the size of a focal adhesion in order to maintain a constant shear stress [21]. In the present theory, we do not try to validate this latter approach, but rather to use it as a basic postulate that is based on the experimental observations in [16, 17], and [22].

When a pair of focal adhesions is only subject to a contractile force, generated by the associated stress fiber, the magnitude of the resultant force sensed by one focal adhesion is equal to that sensed by the other member of the complex; hence, in the absence of external shear, each focal adhesion is expected to have the same size and cross-sectional area. In shear flow, however, a different force is applied to each one of the focal adhesions in a complex; this is because the additional unidirectional shear force induced by the flow increases the total shear in the upstream focal adhesion and, at the same time, partly cancels the total shear in the downstream focal adhesion. This is because the contractile forces on the two focal adhesions in a complex are equal in magnitude and opposite in their direction, while the shear forces on each focal adhesion have the same direction. In order to maintain a constant shear stress in the presence of shear flow (in accord with our basic assumptions discussed in the previous paragraph), this implies that the focal adhesion on the upstream side must have a larger area than the focal adhesion on the downstream side so that the shear, i.e. the ratio of the magnitude of the resultant force to the cross-sectional area in each of the focal adhesions, is equal to an optimal value⁴. This predicted change in focal adhesion size was confirmed in the experiments reported in [22]. These results motivated us to relate the changes in the cross-sectional area of the focal adhesions in a complex to both the contractile force and the

⁴ In [16] it was suggested that the optimal shear is $5.5 \text{ nN } \mu\text{m}^{-2}$.

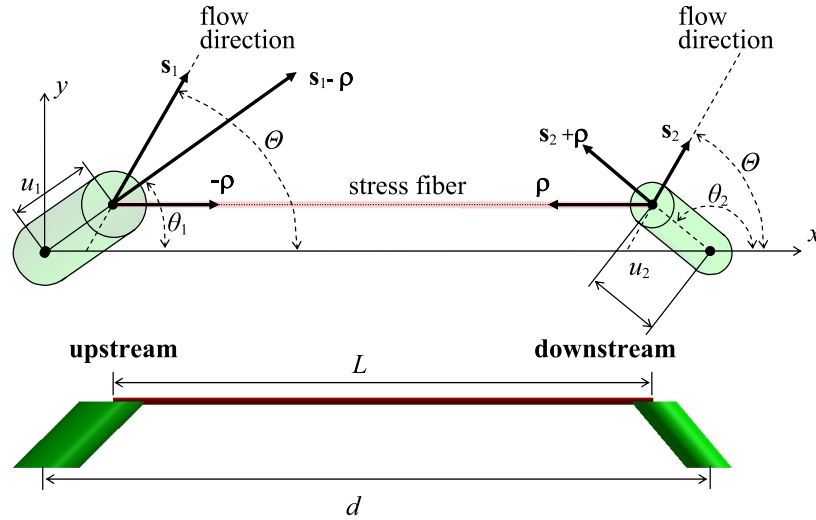


Figure 2. A schematic illustration of a focal adhesion complex. In the upper figure the system is shown from a top view. Each of the focal adhesions is subject to a pure shearing deformation and its elastic response can be thought to be that of a linear spring with a zero stress-free length that is anchored at one end. In its other end the spring is subject to a shear force, s_i , resulting from the flow and a contractile force, ρ . The springs that model the resistance of the focal adhesions to shear are free to rotate and hence, in their equilibrium configuration, they are aligned with the direction of the resultant of the two forces acting on each of them. The variables u_1 and u_2 are the displacements of the upper ends of the focal adhesions; the dimensionless displacements are defined so that $\eta_i = u_i/d$. Because each of the focal adhesions in a complex is subject to a myosin-activated contractile force that acts along the axis of the associated stress fiber, the two focal adhesions are coupled. The forces, ρ , s_1 and s_2 , and the displacements, u_1 and u_2 , are assumed to lie in the plane, $z = \ell$, that is parallel to the x - y plane. A front view of the same configuration of the deformed focal adhesion complex is shown in the bottom figure. When $u_1 = u_2 = 0$ each adhesion will appear as a single circle in a top view.

shear force, and to postulate that the cellular activity not only determines the contractile forces generated by the stress fibers but also changes the cross-sectional area in such a way that, even in the presence of imposed shear, the shear-stress values on each pair of adhesions in a complex are equal.

To account for the effect of the shear flow we assume that the flow results in a homogeneous shear in the cell. The stress field due to such a deformation results in a (shear) force on each focal adhesion that is equal to the (constant) shear, τ , generated by the flow times the (average) cross-sectional area of the focal adhesion. We note that, since a focal adhesion is linked to the substrate on its bottom and to a stress fiber on its top [19], this assumption is reasonable and does not introduce a significant error.

3. Kinematics and theory

We consider a cell plated on a planar substrate that is in the x - y plane of a fixed coordinate system. The direction, \mathbf{n} , of the shear flow makes an angle θ with respect to the positive x direction as shown in figure 2. The heights of the two focal adhesions comprising a complex are assumed, for simplicity, to be fixed and equal to ℓ . We thus only consider displacements in the direction parallel to the plane of the substrate. When a uniform shear is applied, the magnitude of the displacement, u , of a material point in a focal adhesion depends linearly on the distance z from the basal surface:

$$u = \alpha z, \quad (1)$$

where the variable $\alpha = \partial u / \partial z$ is the total strain in each focal adhesion. Hence, to fully determine the deformation

of a focal adhesion it is sufficient to describe the magnitude of the displacement (in a plane normal to the z axis), u , at $z = \ell$ and the direction of this displacement. We here describe the configuration of each member of a pair of focal adhesions by the dimensionless quantity $\eta_i = u_i/d$ characterizing the magnitude of the maximum displacement⁵ and the rotation angle, θ_i , that determines the direction of the displacement as shown in figure 2. The subscript i takes the values 1 or 2, where 1 indicates the focal adhesion that is located in the upstream side of the cell, i.e. the side that is first reached by a moving fluid particle of the induced flow, and 2 indicates the focal adhesion that is in the downstream side. The dimensionless variables $\eta_i = u_i/d$ prescribe the maximum displacement of each of the two focal adhesions, and from equation (1), are equal to $\alpha_i \ell / d$. The distance d between the basal centers of the two focal adhesions and the angle θ that the direction of the flow, \mathbf{n} , makes with the x axis are, for now, taken to be parameters that are fixed in any given experiment. The pair of focal adhesions is subject to a shear stress of magnitude τ exerted on the two termini of the associated stress fiber, and to a contractile force, ρ , exerted by the stress fiber. The distance, L , between the two termini is given by⁶

$$L = |(\mathbf{x}_2 + \mathbf{u}_2) - (\mathbf{x}_1 + \mathbf{u}_1)|. \quad (2)$$

The value of L when the complex is in mechanical equilibrium is smaller than d due to the contractile nature of the stress fiber. The points \mathbf{x}_1 and \mathbf{x}_2 are the barycenters of each of the focal

⁵ In other words, η_i is the horizontal displacement of the upper end of a focal adhesion in units of the length d between the two focal adhesions.

⁶ Notice that coordinate system was chosen so that L is independent of θ .

adhesion's basal surface and are chosen so that \mathbf{x}_1 coincides with the origin and

$$\mathbf{x}_2 = d\mathbf{e}_1. \quad (3)$$

The displacement vectors \mathbf{u}_1 and \mathbf{u}_2 are given by

$$\mathbf{u}_i = d(\eta_i \cos(\theta_i)\mathbf{e}_1 + \eta_i \sin(\theta_i)\mathbf{e}_2), \quad (4)$$

where \mathbf{e}_1 and \mathbf{e}_2 are the unit vectors that denote the positive directions of the x axis and y axis, and the dimensionless displacements are defined so that $\eta_i = u_i/d$. In the absence of shear flow and stress-fiber contractility, $\eta_1 = \eta_2 = 0$ and $L = d$.

In the next section we show how the equations of mechanical equilibrium can be derived from the first variation of the deformation free energy with respect to η_1 , θ_1 , η_2 and θ_2 in which the contributions of the shear forces and the contractile forces are taken into account. Before showing this variational approach (that is essential primarily for a simple determination of the angle θ for which the system is in a globally stable equilibrium) we now give a simpler derivation of the equilibrium configuration of a general complex. We take the angle θ and the forces illustrated as vectors in the complex shown in figure 2 to be fixed. We associate each of the focal adhesions with a linear spring of zero stress-free length and a spring constant, W_i , with $i = 1, 2$ for the upstream and downstream focal adhesions, respectively. Each linear spring is anchored at one end to the rigid substrate and is subject to a shear-flow-induced force \mathbf{s}_i and a contractile force of magnitude ρ as shown in figure 2. When the direction and magnitude of the forces are known, the extension of the spring times the spring constant is equal to the magnitude of the resultant force, and its equilibrium orientation is that of the resultant force, i.e. the vectorial summation of the two external forces. The two springs are coupled in the sense that the forces of contractility on each of them act in opposite directions and lie in the axial line of the stress fiber generating them. However, because the average displacements of the focal adhesions are significantly smaller than the length of the associated stress fiber and are of the order of magnitude of the height of the focal adhesion [20], we assume that the stress fiber remains parallel to the x axis in the deformed configuration. Thus, the balance of forces and moments on each focal adhesion can be expressed as follows:

$$(\mathbf{s}_1 - \boldsymbol{\rho}) \cdot (\cos(\theta_1)\mathbf{e}_1 + \sin(\theta_1)\mathbf{e}_2) = W_1 u_1, \quad (5a)$$

$$\mathbf{u}_1 \times (\mathbf{s}_1 - \boldsymbol{\rho}) = \mathbf{0}, \quad (5b)$$

$$(\mathbf{s}_2 + \boldsymbol{\rho}) \cdot (\cos(\theta_2)\mathbf{e}_1 + \sin(\theta_2)\mathbf{e}_2) = W_2 u_2, \quad (5c)$$

$$\mathbf{u}_2 \times (\mathbf{s}_2 + \boldsymbol{\rho}) = \mathbf{0}. \quad (5d)$$

Equations (5) can be easily written in the form of four independent equations for the four equilibrium values of the kinematical variables u_1 , θ_1 , u_2 and θ_2 . When the direction of the deformed stress fiber is taken to be parallel to the x axis, i.e. when the contractile force $\boldsymbol{\rho}$ is equal to $\rho\mathbf{e}_1$ (with ρ the known magnitude of the myosin-activated contractile force) that system is also uncoupled and can be easily solved, as shown in the next section.

4. Free energy and mechanical equilibrium

To express the energy associated with a focal adhesion complex under shear we use the standard expression⁷ for the elastic energy as a function of the strain and external stress [23]:

$$F = \frac{1}{2}W_1 d^2 \eta_1^2 + \frac{1}{2}W_2 d^2 \eta_2^2 - \tau A_1 \eta_1 d \cos(\theta_1 - \theta) - \tau A_2 \eta_2 d \cos(\theta_2 - \theta) - \rho(L - d), \quad (6)$$

where τ is the shear induced by the flow and A_i , $i = 1, 2$, is the cross-sectional area of each of the focal adhesions that can vary, depending on cell activity. Accordingly, the shear-flow-induced forces (see figure 2) are taken to be $\mathbf{s}_i = \tau A_i (\cos \theta \mathbf{e}_1 + \sin \theta \mathbf{e}_2)$. The energy in (6) takes into account the shear by including the deformation energy given by the product of the shear force and the displacement of the focal adhesion, $\eta_i d$. It is important to note that, because the stress fibers are contractile, the deformed length L is smaller than d . This means that, according to the form of (6), ρ must be negative so that the energy F is decreased as $L - d$ is decreased. The quantities W_1 and W_2 are related to Young's modulus, E , and the area of each adhesion by [24, 25]

$$W_i = \frac{A_i E}{2(1 + \nu)\ell}, \quad (7)$$

where ν is the Poisson ratio of the focal adhesions.

Because the heights of the focal adhesions in a cell are typically three orders of magnitude smaller than the lateral size of a typical stress fiber [20], we further make use of the fact that ℓ/d and hence η_i are significantly smaller than 1. Thus, neglecting terms of higher order, the normalized distance L/d can be approximated from equation (2) as follows:

$$L/d = 1 - \cos(\theta_1)\eta_1 + \cos(\theta_2)\eta_2. \quad (8)$$

This approximation is identical to the assumption, made in the previous section, that the stress fiber in the deformed configuration remains parallel to the x axis. Hence, for ℓ/d , $\eta_i \ll 1$, we can express the modified energy F in (6) of the deformed focal adhesion complex in the following dimensionless form:

$$\hat{F} = \frac{1}{2}(1 - \omega)\eta_1^2 + \frac{1}{2}\omega\eta_2^2 - \lambda(1 - \omega)\eta_1 \cos(\theta_1 - \theta) - \lambda\omega\eta_2 \cos(\theta_2 - \theta) - \hat{\rho}(\cos(\theta_2)\eta_2 - \cos(\theta_1)\eta_1), \quad (9)$$

where the dimensionless variables are defined as follows:

$$\hat{F} = \frac{F}{(W_1 + W_2)d^2}, \quad (10)$$

$$\omega = \frac{A_2}{A_1 + A_2}, \quad \lambda = \frac{2\ell(1 + \nu)\tau}{Ed}, \quad (11)$$

$$\hat{\rho} = \frac{\rho}{(W_1 + W_2)d}.$$

Experiments that measure the dynamics of the cross-sectional area of focal adhesion [22] suggest that the total area of both adhesions, $A_1 + A_2$, is conserved. In the next section we use our basic assumption (based on the

⁷ The parameter ρ can be thought of as a Lagrange multiplier associated with a constraint on the value of $L - d$.

experiments of references [16, 17] and [22]) that the size of each of the focal adhesions in a complex is actively changed in order to achieve an equal value of the shear stress in the upstream and downstream focal adhesions, in order to find the preferred orientation of the complex. We show that under this assumption \hat{F} has a global minimum when the adhesion complex is parallel to the shear flow direction, $\Theta = 0$. This is true for all values of the contractile force and the shear imposed by the flow, characterized by $\hat{\rho}$ and λ , respectively.

We first solve for the equilibrium configuration of a complex for given values of the quantities Θ and ω that vary much more slowly than the degrees of freedom η_1, θ_1, η_2 and θ_2 characterizing the elastic response; those variables reach mechanical equilibrium quickly. We therefore minimize the deformation energy with respect to variations in η_1, θ_1, η_2 and θ_2 . The first variation of \hat{F} with respect to these variables yields the following equilibrium equations that are equivalent to the equations (5)

$$F_{\eta_1} = -(1 - \omega)\lambda \cos(\Theta - \theta_1) + \hat{\rho} \cos(\theta_1) + (1 - \omega)\eta_1, \quad (12a)$$

$$M_{\theta_1} = -((1 - \omega)\lambda \sin(\Theta - \theta_1) + \hat{\rho} \sin(\theta_1))\eta_1, \quad (12b)$$

$$F_{\eta_2} = -\omega\lambda \cos(\Theta - \theta_2) - \hat{\rho} \cos(\theta_2) + \omega\eta_2, \quad (12c)$$

$$M_{\theta_2} = -(\omega\lambda \sin(\Theta - \theta_2) - \hat{\rho} \sin(\theta_2))\eta_2. \quad (12d)$$

The quantities F_{η_i} and M_{θ_i} , $i = 1, 2$, represent the component of the total force along the direction of \mathbf{u}_i and net component along the z axis of the torque⁸ exerted on each of the focal adhesions by the resultant force. Clearly, such force and moment components must vanish if the system can reach mechanical equilibrium. We have confirmed numerically that the following stable solution of the system (12) is indeed the global minimum of the deformation energy (with the approximations mentioned above):

$$\eta_1 = \frac{1}{1 - \omega} \sqrt{(1 - \omega)^2 \lambda^2 + \hat{\rho}^2 - 2(1 - \omega)\lambda\hat{\rho} \cos(\Theta)}, \quad (13a)$$

$$\theta_1 = \tan^{-1} \left(\frac{\sin(\Theta)}{\cos(\Theta) - \hat{\rho}/(\lambda(1 - \omega))} \right), \quad (13b)$$

$$\eta_2 = \frac{1}{\omega} \sqrt{\omega^2 \lambda^2 + \hat{\rho}^2 + 2\omega\lambda\hat{\rho} \cos(\Theta)}, \quad (13c)$$

$$\theta_2 = \tan^{-1} \left(\frac{\sin(\Theta)}{\cos(\Theta) + \hat{\rho}/(\omega\lambda)} \right). \quad (13d)$$

The (normalized) forces originating from the contractility ($\hat{\rho} < 0$), and from the imposed shear flow, characterized by $(1 - \omega)\lambda$ for the upstream and by $\omega\lambda$ for the downstream focal adhesion, are, respectively, parallel to the vectors \mathbf{e}_1 and $\cos \Theta \mathbf{e}_1 + \sin \Theta \mathbf{e}_2$. The (normalized) magnitude of the resultant force exerted on each of the focal adhesions by the shear flow and by the contractility of the stress fibers, i.e. the norm of the vectorial summation of the external forces acting on it, is equal to $\sqrt{(1 - \omega)^2 \lambda^2 + \hat{\rho}^2 - 2(1 - \omega)\lambda\hat{\rho} \cos(\Theta)}$ for the upstream and $\sqrt{\omega^2 \lambda^2 + \hat{\rho}^2 + 2\omega\lambda\hat{\rho} \cos(\Theta)}$ for the downstream focal adhesion. According to the basic assumption described above,

⁸ When the system is not in equilibrium the resultant force may not be aligned with the displacement \mathbf{u}_i .

the cross-sectional area of a focal adhesion is actively changed in order to maintain an optimal value of the effective shear. In terms of our model, an appropriate change in the variable ω (related to the relative areas) would represent this assumed active adjustment of the focal adhesion cross-sectional area as a function of the magnitude of the resultant force exerted on each focal adhesion. The condition of equal shear stresses is therefore given by equating the ratio of the force to the area for each of the adhesions. The expressions for the forces written above show that, when a stress fiber in a complex is oriented parallel to the shear flow, i.e. when $\Theta = 0$, the contractile force exerted on the focal adhesion on the upstream side adds to the force induced by the shear flow, while, for the downstream focal adhesion, the contractile force, at least partly, cancels the shear force since, on that side, the two forces act in opposite directions. The additivity of the contractile and shear forces on the upstream adhesion thus results in an increase in the size of the focal adhesion; on the downstream side, the net force on the adhesion is reduced (since the contractile and shear forces have opposite signs). This results in a reduction of the area of the adhesion on that side. The timescale of the cellular active processes that readjust the size of focal adhesion is of the order of 10 min (see, e.g., [17]). This is several orders of magnitude longer than the timescale for the elastic response of the complex ($\eta_1, \theta_1, \eta_2, \theta_2$) which is given by the size of the adhesion divided by the sound speed in the adhesion. Accordingly, when a complex that is subject to a shear flow in a given orientation, Θ , responds elastically and reaches its equilibrium configuration given by (13) in a timescale that is shorter than that required to reorient the stress fibers, our model requires that the shear stresses (force per unit area) on each adhesion are equal. Using the expression for the force and area, we find that ω must satisfy the following equation:

$$\frac{\sqrt{(1 - \omega)^2 \lambda^2 + \hat{\rho}^2 - 2(1 - \omega)\lambda\hat{\rho} \cos(\Theta)}}{A_1} = \frac{\sqrt{(\omega^2 \lambda^2 + \hat{\rho}^2 + 2\omega\lambda\hat{\rho} \cos(\Theta))}}{A_2}, \quad (14)$$

which, by the first equation in (11) and by (13), implies that the displacements of the two focal adhesions are equal:

$$\eta_1 = \eta_2. \quad (15)$$

The choice of ω so that it satisfies (14) is, here, equivalent to the basic assumption of equal shear in the two focal adhesions in a complex.

5. Results and discussion

The solution of (15) can be written in the form

$$\omega = (1 + \beta \cos(\Theta) + \sqrt{1 + \beta^2 \cos^2(\Theta)})^{-1}. \quad (16)$$

This yields the relative area as a function of the orientation angle for the case where the angle has not yet equilibrated, but the area has reached mechanical equilibrium. In this expression, the positive parameter β is given by

$$\beta = -\frac{\lambda}{\hat{\rho}} = -\frac{\tau(A_1 + A_2)}{\rho}. \quad (17)$$

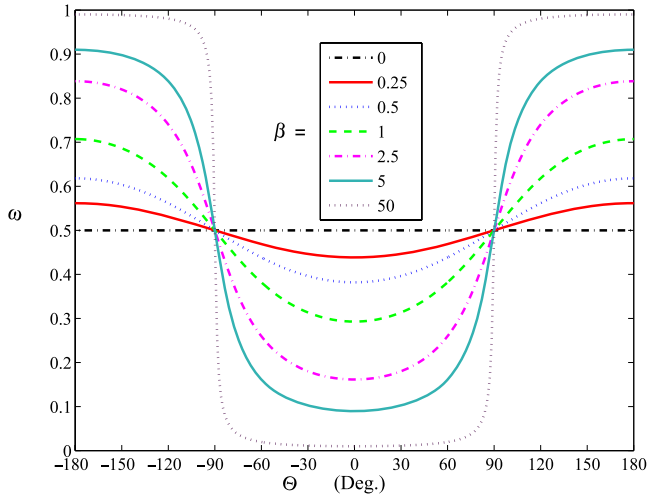


Figure 3. The parameter $\omega = A_2/(A_1 + A_2)$ that measures the relative area in the downstream side focal adhesion versus the flow orientation angle Θ for different values of β which is inversely proportional to the cell contractility.

The dependence of ω on β and the orientation angle Θ is shown in figure 3. The figure shows that, when the shear imposed by the flow is significantly higher than the magnitude of the contractility, the area in the downstream focal adhesion is strongly reduced (and, in the asymptotic limit, tends to zero), while for zero flow rate the areas of the two focal adhesion in a complex are equal, as expected.

When ω is given by (16) and the kinematical variables are in accord with (13), i.e. at their mechanical equilibrium values for which \hat{F} attains its global minimum for given values of $\hat{\rho} < 0$, λ and Θ , the dimensionless free energy is equal to \hat{F}_{eq} ; this can be written in the form

$$\hat{F}_{\text{eq}} = -\frac{1}{2}\hat{\rho} - \hat{\rho}^2 \left(1 + \frac{\beta^2}{2} + \sqrt{1 + \beta^2 \cos(\Theta)^2} \right). \quad (18)$$

The dependence of \hat{F}_{eq} on β and Θ is shown in figure 4. The figure clearly shows that the values of \hat{F} at configurations in the parallel orientation ($\Theta = 0$) are global minima with no bifurcation points for all values of β .

Our treatment up to now looked at the mechanical equilibrium associated with the focal adhesion size and orientation for an imposed, fixed orientation of the stress fibers relative to the applied shear. This is applicable when the timescale associated with focal adhesion growth or shrinkage is much faster than the time for stress-fiber reorientation. At very long times, the stress fibers will reorient as well, in response to the imposed shear. The global equilibrium of the system is then given by the minimization of \hat{F}_{eq} in (18) with respect to the orientation angle of the complex, Θ . Equation (18) shows that the dimensionless free energy, \hat{F}_{eq} , has two extrema at $\Theta = 0$ and $\pi/2$.⁹ The global minimum of \hat{F}_{eq} is obtained when the stress fibers are aligned parallel to the direction of the flow ($\Theta = 0$). The fact that the term that depends on Θ is proportional to $\hat{\rho}^2$ (where $\hat{\rho}$ is a measure of the contractile

⁹ Only at these values of Θ do the forces on the two focal adhesions in a complex yield a vanishing force couple, i.e. a zero net moment.

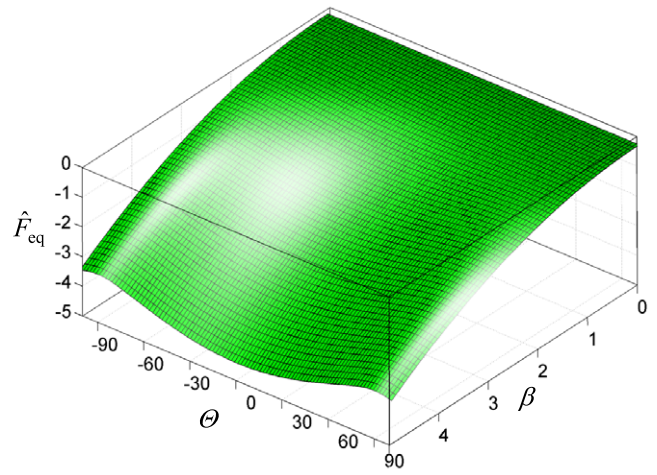


Figure 4. The dimensionless free energy at mechanical equilibrium, \hat{F}_{eq} , as a function of $\beta = -\lambda/\hat{\rho}$ which is inversely proportional to the contractility force, and the orientation angle of the adhesion complex relative to the applied shear, Θ , for $\hat{\rho} = -0.5$.

force per unit area as given by equation (11)) suggests that stress fibers in cells with relatively low contractility (i.e. cells that generate small forces of contraction) may only have a weak tendency to align with the shear flow. For example, noise effects due to Brownian motion, fluctuations of the fibers and other processes might prevent the stress fibers from aligning in systems with small contractile forces. This was also confirmed in a more general model using a simple Metropolis Monte Carlo scheme [26].

An estimate of the order of magnitude of energy differences between the parallel and perpendicular alignment of complexes of cells relative to the direction of the imposed flow can be derived as follows. Following [7, 22] we suppose that the imposed flow yields a shear stress of the order of $20 \text{ dyne cm}^{-2} = 2 \times 10^{-3} \text{ nN } \mu\text{m}^{-2}$. We further estimate the value of the contractile force in fibroblasts to be of the order of 10 nN, as suggested in [16]. Using the data reported in [8] and [16] the total area of all focal adhesions in a cell is around 4% of the complete cellular area. The shear stress that deforms the adhesion is given by the shear force divided by the adhesion area; thus we must divide the average shear stress of the cell of 20 dyn cm^{-2} by 0.04 to estimate the local shear stress on the adhesion. This yields an estimate, $\tau \approx 0.05 \text{ nN } \mu\text{m}^{-2}$, for the flow-induced shear. By taking the area $A_1 + A_2$ to be about $4 \mu\text{m}^2$ we use (17) and (16) to get $\beta \approx 0.02$. To estimate the elastic moduli W_i , we follow an argument given in [20] which gives a lower bound for the displacement of a typical focal adhesion protein as a result of active contractility and assume that, in the presence of shear flow, the displacement of the upper end of a focal adhesion is of the order of its height, i.e. $u_1 = u_2 \approx 100 \text{ nm}$. This yields $W_1 + W_2 \approx 0.1 \text{ nN nm}^{-1}$. With these values, the energy difference, $\Delta F = \rho^2(1 - \sqrt{1 + \beta^2})/(W_1 + W_2)$, between the parallel alignment and the perpendicular alignment of a complex is of the order of $-25k_B T$ at $T = 310 \text{ K}$. We note that in the present theory, for a given shear flow, the value of β characterizing the ratio between the flow-induced shear

force and the contractile force is inversely proportional to the fraction of the cellular area that is covered by focal adhesions, and an increase in this fraction results in a decrease of the absolute magnitude of the energy difference, ΔF , because the local shear stress across a given adhesion is smaller. This suggests that the orientation of complexes in cells that develop a large number of focal adhesions would be nearly independent of θ . An active increase in the total area $A_1 + A_2$ of a complex for which the relative area of the adhesion, ω , is fixed, is equivalent to a decrease in $\hat{\rho}$ and an increase in β . Such changes correspond to an increased tendency of the complex to align with the direction of the flow.

The dynamical scenario that we have presented assumed that the adhesion growth/shrinking kinetics is faster than the focal adhesion complex reorientation. However, in the case where the growth or shrinking kinetics are inhibited (and the areas cannot adjust to the shear) so that there is no active change in the cross-sectional area of each of the focal adhesions in a complex (i.e. ω is fixed), \hat{F}_{eq} is found to be independent of the angle θ :

$$\hat{F}_{\text{eq}} = -\frac{1}{2}\hat{\rho} - \frac{1}{2}\hat{\rho}^2\left(\beta^2 + \frac{1}{(1-\omega)\omega}\right). \quad (19)$$

Equations (18) and (19) suggest that the realignment of stress fibers parallel to the direction of the flow ($\theta = 0$) is indeed driven by the readjustment of the adhesion areas in response to the shear; in the absence of such readjustment, there is no driving force to reorient the stress fibers in response to the applied flow. However, the parallel orientation is favorable only when the cellular activity equalizes the shear stress on each of the focal adhesions in a complex so that ω obeys the relation (16). The dependence of ω on θ in this relation is implied by equation (14), which requires that the two ratios between the total force exerted on each focal adhesion in a complex and its cross-sectional area are equal.

An experimental validation of the results presented above can be achieved by investigating the relation between the contractile strength and the orientational response to shear flow. A controlled reduction in the magnitude of $\hat{\rho}$ will then show the transition from the mechanical regime, characterized by parallel alignment of stress fibers in response to shear, in which cellular noise is negligible, to a regime with no preferred orientation when the magnitude of the contractility, $\hat{\rho}$, is small. The dependence of the mechanical equilibrium configurations on θ and the strength of the imposed shear can possibly be verified using cryo-electron microscopy or atomic force microscopy.

Acknowledgments

We thank the Israel Science Foundation for its support. Part of this research was supported by the historic generosity of the Perlman Family Foundation.

References

[1] De R, Zemel A and Safran S A 2007 Dynamics of cell orientation *Nat. Phys.* **3** 655–9

- [2] Hsu H J, Lee C F and Kaunas R 2009 A dynamic stochastic model of frequency-dependent stress fiber alignment induced by cyclic stretch *PLoS ONE* **4** e4853:1–847
- [3] Brown R A, Prajapati R, McGrouther D A, Yannas I V and Eastwood M 1998 Tensional homeostasis in dermal fibroblasts: mechanical responses to mechanical loading in three-dimensional substrates *J. Cell. Physiol.* **175** 323–32
- [4] Biton Y Y and Safran S A 2009 The cellular response to curvature-induced stress *Phys. Biol.* **6** 046010
- [5] Svitkina T M, Rovinsky Y A, Bershadsky A D and Vasiliev J M 1995 Transverse pattern of microfilament bundles induced in epitheliocytes by cylindrical substrata *J. Cell Sci.* **108** 735–45
- [6] Levina M E, Domnina L V, Rovinsky Y A and Vasiliev J M 1996 Cylindrical substratum induces different patterns of actin microfilament bundles in nontransformed and in ras-transformed epitheliocytes *Exp. Cell Res.* **229** 159–65
- [7] Owatverot T B, Oswald S J, Chen Y, Wille J J and Yin F C-P 2005 Effect of combined cyclic stretch and fluid shear stress on endothelial cell morphological responses *J. Biomech. Eng.* **127** 374–82
- [8] Li S, Butler P, Wang Y, Hu Y, Han D C, Usami S, Guan J L and Chien S 2002 The role of the dynamics of focal adhesion kinase in the mechanotaxis of endothelial cells *Proc. Natl Acad. Sci.* **99** 3546–51
- [9] Davies P F, Robotewskyj A and Griem L 1994 Quantitative studies of endothelial cell adhesion: directional remodeling of focal adhesion sites in response to flow forces *J. Clin. Invest.* **93** 2031–8
- [10] Noria S, Cowan D B, Gotlieb A I and Langille B L 1999 Transient and steady-state effects of shear stress on endothelial cell adherens junctions *Circ. Res.* **85** 504–14
- [11] Bresnick A R 1999 Molecular mechanisms of nonmuscle myosin-ii regulation *Curr. Opin. Cell Biol.* **11** 26–33
- [12] Nicolas A, Geiger B and Safran S A 2004 Cell mechanosensitivity controls the anisotropy of focal adhesions *Proc. Natl Acad. Sci. USA* **101** 12520–5
- [13] Shemesh T, Geiger B, Bershadsky A D and Kozlov M M 2005 Focal adhesions as mechanosensors: a physical mechanism *Proc. Natl Acad. Sci. USA* **102** 12383–8
- [14] Besser A and Safran S A 2006 Force-induced adsorption and anisotropic growth of focal adhesions *Biophys. J.* **90** 3469–84
- [15] Deshpande V S, Mrksich M, McMeeking R M and Evans A G 2008 A bio-mechanical model for coupling cell contractility with focal adhesion formation *J. Mech. Phys. Solids* **56** 1484–510
- [16] Balaban N Q, Schwarz U S, Riveline D, Goichberg P, Tzur G, Sabanay I, Mahalu D, Safran S A, Bershadsky A D, Addadi L and Geiger B 2001 Force and focal adhesion assembly: a close relationship studied using elastic micropatterned substrates *Nat. Cell Biol.* **3** 466–72
- [17] Tan J L, Tien J, Pirone D M, Gray D S, Bhadriraju K and Chen C S 2003 Cells lying on a bed of microneedles: an approach to isolate mechanical force *Proc. Natl Acad. Sci. USA* **100** 1484–9
- [18] Raz-Ben Aroush D and Wagner H D 2006 Shear-stress profile along a cell focal adhesion *Adv. Mater.* **18** 1537–40
- [19] Raz-Ben Aroush D, Zaidel-Bar R, Bershadsky A D and Wagner H D 2008 Temporal evolution of cell focal adhesions: experimental observations and shear stress profiles *Soft Matter* **4** 2410–7
- [20] Bershadsky A D, Kozlov M M and Geiger B 2006 Adhesion-mediated mechanosensitivity: a time to experiment, and a time to theorize *Curr. Opin. Cell Biol.* **18** 472–81
- [21] Bershadsky A D, Balaban N Q and Geiger B 2003 Adhesion-dependent cell mechanosensitivity *Annu. Rev. Cell Dev. Biol.* **19** 677–95

- [22] Zaidel-Bar R, Kam Z and Geiger B 2005 Polarized downregulation of the paxillin-p130cas-rac1 pathway induced by shear flow *J. Cell Sci.* **118** 3997–4007
- [23] Thompson J M T and Hunt G W 1973 *A General Theory of Elastic Stability* (London: Wiley)
- [24] Landau L D and Lifshitz E M 1970 *Theory of Elasticity* (Oxford: Pergamon)
- [25] Love A E H 1927 *A Treatise on the Mathematical Theory of Elasticity* (New York: Dover)
- [26] Metropolis N, Rosenbluth A W, Rosenbluth M N, Teller A H and Teller E 1953 Equation of state calculations by fast computing machines *J. Chem. Phys.* **21** 1087–92